HHS Public Access

Author manuscript

Nat Cell Biol. Author manuscript; available in PMC 2021 April 05.

Published in final edited form as:

Nat Cell Biol. 2019 July ; 21(7): 824–834. doi:10.1038/s41556-019-0342-1.

Whsc1 links pluripotency exit with mesendoderm specification

Tian V. Tian[1], **Bruno Di Stefano**[1,3], **Grégoire Stik**[1], **Maria Vila-Casadesús**[1], **José Luis Sardina**[1], **Enrique Vidal**[1], **Alessandro Dasti**[1], **Carolina Segura Morales**[1], **Luisa De Andres Aguayo**[1], **Antonio Gomez**[1], **Johanna Goldmann**[1,4], **Rudolf Jaenisch**[4,5], **Thomas Graf**[1,2]

[1]Center for Genomic Regulation (CRG), The Barcelona Institute of Science and Technology, Carrer Dr Aiguader 88, 08003 Barcelona, Spain

[2]Universitat Pompeu Fabra (UPF), Barcelona, Spain

[3]Department of Stem Cell and Regenerative Biology, Harvard University, Cambridge, MA 02138, USA

[4]The Whitehead Institute for Biomedical Research, 9 Cambridge Center, Cambridge, MA 02142, USA

[5]Department of Biology, Massachusetts Institute of Technology, 31 Ames Street, Cambridge, MA02139, USA

Abstract

How pluripotent stem cells differentiate into the main germ layers is a key question of developmental biology. Here we show that the chromatin-related factor Whsc1 (Nsd2, MMSET) has a dual role in pluripotency exit and germ layer specification of embryonic stem cells (ESCs). Upon induction of differentiation, a proportion of Whsc1-depleted ESCs remain entrapped in a pluripotent state and fail to form mesendoderm, although they are still capable of generating neuroectoderm. These functions of Whsc1 are independent of its methyltransferase activity. Whsc1 binds to enhancers of the mesendodermal regulators *Gata4*, *T* (*Brachyury)*, *Gata6* and *Foxa2* together with Brd4, and activates the genes' expression. Depleting each of these regulators also delays pluripotency exit, suggesting that they mediate the effects observed with Whsc1. Our data indicate that Whsc1 links silencing of the pluripotency regulatory network with activation of mesendoderm lineages.

Keywords

Whsc1; chromatin related factor; embryonic stem cells; pluripotency exit; germ layer specification; Brd4

Correspondence: thomas.graf@crg.eu, tian.tian@crg.eu.

Author Contributions

T.V.T and T.G. conceived the project, designed the experimental work and wrote the manuscript. T.V.T, B.D.S., G.S. A.D., J.L.S., C.S.M. L.D.A.A. and J.G. performed the experiments. R.J. provided reagents. E.V., M.V.C. and A.G. conducted the bioinformatics analysis.

Competing interests

R.J. is an advisor/co-founder of Fate Therapeutics, Fulcrum Therapeutics, and Omega Therapeutics and Dewpoint Therapeutics.

Introduction

Embryonic stem cells (ESCs) are an excellent model to study the generation of the three main germ layers, endoderm, mesoderm and ectoderm [1]. The first event during the transition of ESCs into more differentiated cells is the exit from pluripotency, which includes silencing of the core pluripotency transcription factors (TFs) Oct4, Sox2 and Nanog [2–4]. This process can either be externally initiated by deprivation of self-renewal signals [5] or by exposure of the cells to differentiation-inducing cues [6]. Subsequently, germ layer-instructive TFs become up-regulated and activate markers that define the various lineages [4]. These factors comprise Brachyury (T) and Gata4 for mesoderm, Gata6, Gata4 and Foxa2 for endoderm and Pax6 and Sox1 for neuroectoderm [3, 4, 6, 7]. Screens with ESC reporter lines and haploid ESCs have identified several regulators required for pluripotency exit, including several TFs and RNA binding proteins, all of which were shown to affect members of the pluripotency network [8–13].

Besides TFs and noncoding RNAs, chromatin-related factors (CRFs) play an important role in ESC differentiation, which involves a progressive transition from a relatively open chromatin state to a more compact one [14]. Several CRFs are broadly involved in ESC differentiation, such as Polycomb group proteins that are required for the repression of pluripotency associated and lineage inappropriate genes [15]. Others act in a more restricted fashion, as exemplified by the requirement of Setd2 for endodermal [16], Mel18 for mesodermal [17] and Zrf1 for neuroectodermal differentiation [18].

Here we report that Whsc1 is required for efficient pluripotency exit and mesendoderm specification, independent of its methyltransferase activity. These effects can be explained by its ability to activate several mesendoderm regulators.

Results

Whsc1 is required for efficient exit from pluripotency

To search for CRFs that play a role in pluripotency exit and subsequent ESC differentiation we performed an *in-silico* screen by analysing datasets that record transcriptome changes during the differentiation of mouse ESCs into embryoid bodies (EBs). We compiled a list of 653 genes encoding histone writers and readers, histone variants, nucleosome positioning proteins and a selection of long non-coding RNAs (Supplementary Table 1 and Supplementary Fig. 1a). Three candidates consistently scored among the most up-regulated genes. These were *Cbx4,* encoding a Polycomb group protein that has been shown to orchestrate ESC differentiation [19], *L3mbtl3*, a putative Polycomb group family member [20] and *Whsc1*, encoding a SET-domain methyltransferase which in humans is associated with Wolf-Hirschhorn syndrome [21].

To study whether these candidates are required for pluripotency exit we tested the effects of knockdowns on the differentiation of a pluripotency reporter ESC line. This line, which contains a destabilized version of GFP knocked into the *Rex1* locus (Rex1GFPd2) [8], was induced to differentiate by transfer into medium containing N2 and B27 supplements, Activin A and foetal bovine serum (FBS) [22, 23]. Upon induction, the reporter line became

GFP negative within 48–72h (Fig. 1a–c) confirming that the loss of Rex1 expression is a highly sensitive readout for exit from the pluripotent state [24, 25]. Concomitantly, the cells down-regulated pluripotency associated genes and up-regulated mesendoderm and neuroectoderm specific genes (Supplementary Fig. 1b).

Two independent small hairpin RNA (shRNA) lentiviral constructs were used to knock down the expression of each of the three candidate genes. After induction of differentiation, cells expressing scrambled shRNA (shScr) became GFP negative within 48–72h post induction (p.i.), as did cells expressing shCbx4 and shL3mbtl3 (Supplementary Fig. 1c). In contrast, 25–35% of ESCs transduced with the shWhsc1 constructs retained GFP expression (Fig. 1b, c). Notably, both Whsc1 knockdown constructs strongly reduced the expression of both Whsc1 mRNA and the ~180 and ~100kDa protein isoforms (Fig. 1d). Interestingly, shWhsc1 ESCs retained elevated expression levels of the pluripotency genes *Rex1, Pou5f1, Nanog, Lin28a* and *Esrrb* (Fig. 1e). In addition, Whsc1-depleted cells, when re-plated after induced differentiation, yielded large numbers of colonies positive for alkaline phosphatase (AP, an indicator of pluripotency) even after 2 consecutive rounds of treatment, whereas no such colonies could be recovered from control cells as early as after one round (Supplementary Fig. 1d). Depletion of Whsc1 in ESCs neither resulted in an up-regulation of pluripotency factors nor in an alteration of the cells' growth kinetics (Supplementary Fig. 1e–g), ruling out more indirect effects on pluripotency exit.

In summary, Whsc1 depletion impaired the down-regulation of pluripotency markers, indicating a requirement for efficient pluripotency exit.

Depletion of Whsc1 impairs induction of mesendoderm differentiation *in vitro* and *in vivo*

To evaluate the effect of Whsc1 depletion on the differentiation capacity of ESCs, we examined embryoid bodies (EBs) derived from knockdown ESCs (Fig. 2a). Whsc1-depleted EBs were smaller than those from control ESCs (Fig. 2b), exhibited lower levels of Whsc1 mRNA and protein while retaining pluripotency factor expression (Fig. 2c, d). Importantly, Whsc1-depleted EBs also showed a strongly reduced expression of the mesendoderm regulator genes *Gata4*, *T*, *Gata6*, *Foxa2, Sox17* and *Flk1*, while neuroectodermal gene expression (*Sox1*, *Pax6* and *Nes*) remained unaffected (Fig. 2c). In addition, when shWhsc1 EBs were dissociated and re-plated onto mouse embryo fibroblasts (MEFs) in medium with 2i and LIF they formed large numbers of AP positive colonies, whereas control cells yielded few such colonies (Fig. 2e), suggesting that shWhsc1 EBs retained pluripotent cells. Moreover, EBs derived from shWhsc1 Epiblast Stem Cells (EpiSCs) also retained *Pou5f1* expression and showed reduced developmental potential towards the mesendoderm lineage (Supplementary Fig. 2a).

To probe their differentiation potential *in vivo*, we generated teratomas in immunodeficient mice. Control cell-derived teratomas contained tissues from all three germ layers, including muscle, cartilage, gut epithelium and neuro-epithelium. In contrast, Whsc1-depleted teratomas derived were mainly composed of neuro-epithelium and poorly differentiated cells (Supplementary Fig. 2b). Accordingly, shWhsc1 teratomas retained pluripotency and neuroectoderm marker expression while showing reduced levels of mesendoderm markers (Supplementary Fig. 2c).

Since both EBs and teratomas comprise a complex mixture of cells, we next tested the effects of Whsc1 knockdown on the directed differentiation of ESCs towards mesoderm, endoderm and ectoderm. Whsc1-depleted cells generated significantly fewer beating cardiomyocyte-containing colonies than control cells (Supplementary Fig. 3a, Supplementary Movie 1, 2) and a reduced expression of the cardiac regulators *Mef2c* and *Nkx2.5* at 10 days p.i., while exhibiting increased *Rex1* and *Pou5f1* expression (Supplementary Fig. 3b, c). To test the effects of shWhsc1 on definitive endoderm differentiation, Eomes-GFP reporter ESCs [26] were transferred into medium containing Activin A, Fgf4, heparin, PI-103 and CHIR [27]. Seven days later about 30% of control cells became GFP positive, whereas only 5% of Whsc1-depleted cells did so (Supplementary Fig. 3d, e). In line with these findings, shWhsc1-expressing cells showed impaired up-regulation of the endoderm markers *Cxcr4, Cldn6, Foxa2, Gata6* and *Sox17* and inefficient down-regulation of the pluripotency regulators *Rex1*, *Pou5f1* and *Esrrb* (Supplementary Fig. 3f, g). Finally, we derived neural progenitor cells [28] from control and *Whsc1* knockdown ESCs and found no significant differences in the expression of the neural markers *Pax6, Sox1* and *Nes* nor that of *Pou5f1* and *Esrrb* (Supplementary Fig. 3h).

Taken together, the results obtained with embryoid bodies, teratomas and directed germ layer induction experiments confirm that the delay of pluripotency exit induced by Whsc1-depletion is coupled to an impairment of mesendoderm differentiation.

The catalytic SET-domain of Whsc1 is dispensable for efficient pluripotency exit and mesendoderm differentiation

Whsc1 requires the catalytic SET-domain on the C-terminus to di-methylate the lysine 36 on histone 3 (Supplementary Fig. 4a) [29, 30]. This function has been linked to the normal foetal heart and cartilage development in a murine model in which the SET-domain of Whsc1 was excised [31]. Surprisingly, however, ESCs derived from these mice (hereafter referred to as ΔSET) behaved like WT ESCs in our assays (Supplementary Fig. 4b, c). In contrast, expression of shWhsc1.4 which targets the 5' end of Whsc1 mRNA in ΔSET ESCs caused a delay in pluripotency exit, and EBs derived from these cells also showed the retention of pluripotency gene expression and the selective reduction of mesendoderm marker expression (Supplementary Fig. 4b, c). As the *Whsc1* gene produces two major transcripts encoding a full-length protein of ~180kD and a short isoform of ~100kD that corresponds to the N-terminal portion (Fig. 3a), we examined Whsc1 expression by Western blot. We found that ΔSET ESCs also express two proteins: the larger protein corresponds to a C-terminal truncated form of ~130kD and the 100kD isoform (Supplementary Fig. 4, d). These results raise the possibility that in the absence of catalytic SET domain, the N-terminus of Whsc1 plays a role in both the induction of pluripotency exit and mesendoderm specification.

To explore this hypothesis, we used a CRISPR-Cas9 approach to generate an ESC line with a complete *Whsc1* knockout, by targeting exon1 and exon15. This led to the deletion of a ca. 40Kb fragment encoding both the long and short isoforms of *Whsc1* (Fig. 3a) and also eliminated multiple AUGs that could serve as potential start codons. *Whsc1*−/− ESCs lacked both protein isoforms (Fig. 3b), expressed unaltered levels of *Sox2, Oct4* and *Nanog* (Fig. 3b) and showed a delayed down-regulation of *Rex1*, *Pou5f1* and *Nanog* after differentiation

induction (Fig. 3c). EB derivatives were impaired in the up-regulation of mesendoderm but not of neuroectoderm genes and exhibited a delayed down-regulation of *Rex1, Pou5f1* and *Nanog* (Fig. 3d).

To test the possibility that the observed phenotype of *Whsc1−/−* cells could be explained by alterations already pre-existing in the ESCs caused by the knockout, we performed an RNA-seq analysis and found no significant expression changes of pluripotency genes *Pou5f1, Sox2, Nanog, Esrrb and Rex1* compared to *Whsc1+/+* ESCs. Moreover, only 71 genes were found to be differentially expressed in *Whsc1−/−* cells (Fig. 3e). Of note, this list did not include factors described to dismantle the pluripotency network, such as *Flcn*, *Tcf3, Zfp706, Foxd3, Mettl3* and *Pum1* [8–13, 32] (Supplementary Table 2).

In sum, our data show that the SET domain is dispensable for the ability of Whsc1 to facilitate rapid pluripotency exit and to induce mesendoderm specification.

The N-terminus of Whsc1 is sufficient to induce pluripotency exit and mesendoderm differentiation

In an attempt to show that the N-terminal domain of Whsc1 is sufficient for the biological properties of *Whsc1−/−* ESCs we performed rescue experiments. For this, we engineered Flag tagged constructs of full length human WHSC1 (FL), two N-terminal fragments of different lengths (Nter-1 and 2) and a C-terminal portion containing the SET-domain (Cter) (Fig. 4a). *Whsc1−/−* cells expressing these constructs were subjected to the pluripotency exit and germ layer formation assays; as expected, FL-WHSC1 rescued the cell's phenotype in both assays (Fig. 4b, c). Remarkably, expression of either N-terminal construct (Nter-1 and 2) in *Whsc1 −/−* cells was sufficient to rescue the cells' phenotype, showing rapid down-regulation of *Rex1, Pou5f1* and *Nanog* after induction of differentiation. In contrast, the C-terminal construct containing the SET domain failed to rescue (Fig. 4b). In line with these findings, expression of either N-terminal construct was also sufficient to restore mesendoderm marker up-regulation and pluripotency gene down-regulation during EB formation, while the C-terminal construct showed no such effect (Fig. 4c). Since Whsc1 has been described to methylate H3K36 and to alter EZH2 binding in multiple myeloma cells [29, 30], we compared *Whsc1+/+* and *Whsc1−/−* ESCs for the relevant histone marks. However, we found no significant differences in the global levels of H3K36me2, H3K36me3 and the EZH2-associated H3K27me3 mark (Supplementary Fig. 4e).

Our findings show that the N-terminus of Whsc1 is sufficient to facilitate rapid exit from pluripotency and induce mesendoderm formation. They also suggest that the methyltransferase activity of Whsc1 acts in a cell context-dependent manner.

Whsc1 mediates enhancer activation of mesendoderm regulators

Our observations raise the possibility that Whsc1 directly controls the expression of transcription factors that specify mesodermal and endodermal lineages. We therefore asked whether Whsc1 binds to and activates mesendodermal specific enhancers. We focused on genomic loci of the mesendoderm-instructive TF genes *Gata4*, *T*, *Gata6*, and *Foxa2*. Putative enhancers of the neuroectodermal TF genes *Pax6* and *Sox1* were included as controls. To identify candidate regulatory regions of these genes, we mapped the distribution of the

enhancer mark H3K27ac in cells either positive for the mesendodermal markers Eomes or Flk1, in mesendodermal progenitors induced by Activin A, and in neural progenitor cells. In addition, as it has been shown that promoter-enhancer interactions occur mainly within the same Topologically Associating Domains (TADs) [33, 34], we focused on regions within the same TAD. These analyses revealed the presence of several putative enhancers selectively marked by H3K27ac in either mesendodermal or neuroectodermal cells (Fig. 5a and Supplementary Fig. 5a). To explore whether Whsc1 binds to these regions, we performed ChIP analyses using day 6 (D6) EBs. This showed that Whsc1 is significantly enriched at 8 out of 26 putative enhancers tested within the *T*, *Gata6*, *Foxa2* and *Gata4* loci and that this enrichment is reduced in *Whsc1−/−* EBs (Fig. 5b and Supplementary Fig. 5b). Notably, no significant Whsc1 binding was observed in 12 regions specifically marked by H3K27ac in the *Pax6* and *Sox1* loci in ectodermal cells (Supplementary Fig. 5b). To further explore whether these Whsc1-bound regulatory regions are required for target gene regulation, we performed UMI-4C experiments using promoter regions of *T, Gata6, Foxa2* and *Gata4* as viewpoints in ESCs and D6 EBs, comparing *Whsc1+/+* and *−/−* cells. We found that most Whsc1-bound putative mesendodermal enhancers appear to interact with target gene promoter regions in *Whsc1+/+* D6 EBs but not in ESCs, and that these contacts are lost/decreased in *Whsc1−/−* D6 EBs (Fig. 5c and Supplementary Fig. 5c). These observations are consistent with the notion that the relevant regions are involved in Whsc1 mediated target gene regulation.

To test whether Whsc1 binding is associated with enhancer activity, we monitored H3K27ac enrichment at Whsc1-bound regions in *Whsc1*+/+ and −/− D6 EBs within the *T, Gata6, Foxa2* and *Gata4* loci. Regions not bound by Whsc1 served as controls. All 10 Whsc1-bound regions showed a significant decrease of H3K27ac decoration in the *Whsc1−/−* cells. In contrast, in the same cells 14 out of 16 regions not bound by Whsc1 and all 12 sites within the *Sox1* and *Pax6* regions tested showed no significant H3K27ac change (Fig. 5d and Supplementary Fig. 5d). Similar results were obtained for the H3K4me2 mark (Supplementary Fig. 5e). In addition, the 10 Whsc1-bound regions showed no significant binding of Whsc1 in ESCs (Supplementary Fig. 5f) and their H3K27ac enrichment in ESCs was lower than in D6 EBs (Supplementary Fig. 5f).

Taken together, these data show that Whsc1 binding is associated with active enhancers of target genes.

Whsc1 interacts with Brd4 to facilitate activation of mesendoderm enhancers

The bromodomain protein Brd4 has been reported to be required for enhancer activation and gene expression [35] and to interact with Whsc1 [36]. We therefore tested whether Brd4 interacts with Whsc1 at the enhancer regions described above (Fig. 5b and Supplementary Fig. 5b). We found that in D6 *Whsc1+/+* EBs Brd4 indeed binds to the enhancers of *T*, *Gata6*, *Foxa2* and *Gata4* as well as to those of *Sox1* and *Pax6*. Importantly, Brd4 binding was significantly decreased in *Whsc1−/−* EBs at the mesendoderm enhancers but not at the ectoderm enhancers (Fig. 6a). In addition, EBs treated during their formation with the Brd4 inhibitor JQ1 [37] showed reduced expression of the mesendodermal regulator genes *Gata4*, *T*, *Gata6* and *Foxa2*, compared to DMSO treated control EBs (Fig. 6b). We also observed an increase

of neuroectoderm markers *Sox1*, *Pax6* and *Nestin* in JQ1-treated EBs, in line with the reported induction of neural differentiation after Brd4 depletion in ESCs [38] (Fig. 6c). Moreover, both Whsc1 isoforms were found to co-immunoprecipitate with Brd4 in D6 EB extracts (Fig. 6d), consistent with the notion that the N-terminus of Whsc1 is sufficient for this interaction.

Together, our results show that Whsc1 interacts with Brd4, and that this interaction favours the activation of mesendoderm enhancers but not of ectoderm enhancers.

Gata6 recruits Whsc1 to a subset of mesendodermal enhancers

We next asked whether mesendoderm specific regulators are also able to interact with Whsc1 and recruit the factor to their target sites. As a model, we chose to study Gata6 and first performed co-immunoprecipitation experiments. Indeed, both long and short Whsc1 isoforms co-immunoprecipitate with Gata6 in D6 EBs, suggesting that the SET domain, not contained in the 100kDa isoform, is dispensable for this interaction (Fig. 6e). To probe the second question, we generated *Gata6* knockout ESCs by CRISPR-Cas9 mediated genome editing. These cells retain an ESC-like phenotype when grown in LIF- and 2i- containing medium. The *Gata6*$^{-/-}$ ESCs were then used to generate EBs and to perform Whsc1 ChIP experiments in D4 EBs. We tested all 10 previously identified Whsc1-bound enhancer regions of *T*, *Gata4*, *Gata6* and *Foxa2* and found significantly decreased binding of Whsc1 at 6 of these regions (Fig. 6f).

These findings suggest that the mesendodermal lineage specifier Gata6 is capable of recruiting Whsc1 to a subset of mesendoderm specific enhancers.

Depletion of mesendoderm TFs in ESCs causes a delay in pluripotency exit

The finding that Whsc1 is associated with the activation of *Gata4*, *T, Gata6*, and *Foxa2* during ESC differentiation raised the possibility that the encoded mesendoderm instructive TFs are downstream mediators of Whsc1 in pluripotency exit and germ layer specification. To test this hypothesis, we transfected Rex1GFPd2 ESCs with siRNAs against *Gata4*, *T*, *Foxa2* and *Gata6,* respectively, resulting in significant downregulation of the genes (Supplementary Fig. 6a). The cells were then induced to differentiate by transfer into N2B27 medium containing Activin A and FBS. While control siRNA cells showed a complete loss of GFP expression at 48 hours p.i., a significant proportion of cells transfected with siRNAs against *Gata6, T*, *Gata4* and *Foxa2* remained GFP positive (Supplementary Fig. 6b). To further study the role of these factors in pluripotency exit, we tested *Gata6* and *Foxa2* knockout ESCs generated by CRISPR-Cas9-mediated genome editing. Monitoring gene expression at different times after induction of differentiation revealed that, as for *Whsc1*$^{-/-}$ cells, *Gata6*$^{-/-}$ and *Foxa2*$^{-/-}$ cells showed a delayed down-regulation of the pluripotency genes *Oct4*, *Rex1* and *Nanog* (Fig. 7a). The retention of Oct4 and Nanog expression in *Gata6* and *Foxa2* knockout cells was also confirmed at the protein level in cells induced to differentiate for 72 hours (Fig. 7b). Moreover, when these cells were induced to generate EBs, they showed a delayed down-regulation of pluripotency markers similar to that found with *Whsc1*$^{-/-}$ EBs (Fig. 7c)

In conclusion, our data have shown that the depletion or knockout in ESCs of the mesendoderm regulators *Gata6, T*, *Gata4* and *Foxa2* downstream of Whsc1 delays pluripotency exit.

Discussion

Here we describe that the chromatin-related factor Whsc1 has a role in both pluripotency exit and germ layer specification of ESCs. Depletion of Whsc1 entraps the cells in a pluripotent state and inhibits their specification towards mesoderm and endoderm lineages, without impairing neuro-ectoderm formation. Mechanistically, Whsc1 binds to and activates enhancers of mesendoderm lineage-instructive TFs during lineage specification, independently of its methyltransferase activity mediated by the SET-domain. Moreover, depletion of downstream mesendodermal regulators also delayed pluripotency exit, explaining, at least in part, the effects observed after Whsc1 ablation.

Several factors previously described to be required for pluripotency exit have been shown to dismantle directly the pluripotency-associated regulatory network. Hence, folliculin together with its interaction partners Fnip1/2 sequesters the pluripotency associated TF Tfe3 in the cytoplasm [13]; the TFs Tcf3, Foxd3 and Zfp706 repress pluripotency gene expression [8–11]; and the RNA binding proteins Mettl3 and Pum1 destabilize pluripotency gene transcripts [11, 12, 32]. In contrast, we have found that Whsc1 does not act primarily on the pluripotency network, but controls the up-regulation of mesendodermal regulators, including Gata4, T, Gata6 and Foxa2, which on their own also control pluripotency exit. Our observations suggest that the regulatory networks controlling pluripotency and germ layer specification are intimately linked. Indeed, several studies have shown that during murine gastrulation in the primitive streak the pluripotency factors Nanog, Oct4 and Sox2 are co-expressed with the mesendoderm lineage factors T [39], Gata6 [40] and Foxa2 [41]. Moreover, it has been shown that pluripotency TFs are crucial for the up-regulation of germ layer genes upon differentiation, as differentiation fails when pluripotency TFs are acutely ablated [7, 42–44]. In addition, one study also suggests that during *in vitro* differentiation of ESCs GATA6 represses pluripotency factor expression [45].

Our findings support the notion that Whsc1 is recruited to chromatin by lineage regulators. Thus, co-immunoprecipitation experiments showed that Whsc1 interacts with Gata6 and that it loses its ability to bind to most of the mesendodermal enhancers in Gata6 deficient embryoid bodies. It is possible that other sites bound by Whsc1 additional regulators are operative, such as has been described for Nkx2.5 in cardiac cells [31]. Our study also showed an interaction between Whsc1 and the transcriptional co-activator Brd4 in EBs, supporting earlier studies [36]. Moreover, EBs lacking Whsc1 showed a reduced binding of Brd4 specifically at mesendodermal enhancers suggesting that Whsc1 facilitates the recruitment of Brd4 to these enhancers, leading to their activation. The finding that the BRD4 inhibition by BET inhibitor JQ1 impairs the upregulation of mesendoderm regulators while dramatically enhancing the expression of ectodermal regulators supports previous observations in ESCs [38]. Together, our data suggest that Whsc1 enables Brd4 to act as a coactivator of mesendodermal enhancers.

In certain forms of cancer, including multiple myeloma and acute lymphoblastic leukaemia, WHSC1 has been found to be either overexpressed or hyper-activated, resulting in an increased methylation of H3K36 on promoters of oncogenes that drive the disease [29, 30, 46]. This is mediated by the methyltransferase activity of the SET-domain. In contrast, a short isoform of NSD3 (another member of the Nsd family), lacking the SET-domain, can act together with Brd4 on enhancers of genes that drive acute myeloid leukemia [47]. Interestingly, the PWWP domain responsible for this interaction is highly conserved between members of the Nsd family, and in Whsc1 it is located within the N-terminus that interacts with Brd4 [48].

Wolf-Hirschhorn syndrome patients with *WHSC1* deletions often exhibit symptoms characteristic of midline defects, including craniofacial malformations and heart defects [49]. These features have been attributed to the SET-domain of the protein, since mice lacking this domain of Whsc1 largely reflect this phenotype, exhibiting aberrant craniofacial, cardiac and cartilage structures [31, 50]. It will now be interesting to elucidate whether the function of Whsc1 described here is also involved in gene regulation during embryo development, cardiogenesis and cancer.

Supplementary Material

Refer to Web version on PubMed Central for supplementary material.

Acknowledgements

We would like to thank A. Smith for providing the Rex1GFPd2 cells, K. Nimura for the Whsc1 ΔSET cells, E. J. Robertson for the Eomes-GFP cells, A. Surani for the X^{GFP} EpiSCs, J. E. Bradner for the JQ1 compound; L. Batlle, C. Berenguer for technical help; the CRG core facilities flow cytometry, advanced light microscopy and tissue engineering; L. Di Croce, B. Payer, M. Behringer, J. Licht, K. M. Loh, K. Kaji and R. Stadhouders for advice and discussions. T.V.T. and J.L.S. were supported by Juan de la Cierva postdoctoral fellowships (MINECO, FJCI-2014-22946 and IJCI-2014-21872), B.D.S. by an EMBO long-term fellowship (#ALTF 1143-2015), G.S. by a Marie Sklodowska-Curie fellowship, J.G. by a Boehringer Ingelheim Graduate Student Fellowship. R.J. was supported by NIH grants R01 NS088538-01 and 2R01MH104610-15. This work was supported by the EU-FP7 project BLUEPRINT, the Spanish Ministry of Economy, Industry and Competitiveness (MEIC) to the EMBL partnership, Centro de Excelencia Severo Ochoa 2013–2017 and the CERCA Program Generalitat de Catalunya. T.V.T, J.L.S. and B.D.S were supported by a CRG award for junior collaborative projects.

References

1. Nichols J & Smith A The origin and identity of embryonic stem cells. Development 138, 3–8 (2011). [PubMed: 21138972]
2. Jaenisch R & Young R Stem cells, the molecular circuitry of pluripotency and nuclear reprogramming. Cell 132, 567–582 (2008). [PubMed: 18295576]
3. Young RA Control of the embryonic stem cell state. Cell 144, 940–954 (2011). [PubMed: 21414485]
4. Martello G & Smith A The nature of embryonic stem cells. Annu Rev Cell Dev Biol 30, 647–675 (2014). [PubMed: 25288119]
5. Clevers H, Loh KM & Nusse R Stem cell signaling. An integral program for tissue renewal and regeneration: Wnt signaling and stem cell control. Science 346, 1248012 (2014). [PubMed: 25278615]
6. Loh KM, Lim B & Ang LT Ex uno plures: molecular designs for embryonic pluripotency. Physiol Rev 95, 245–295 (2015). [PubMed: 25540144]

7. Loh KM & Lim B A precarious balance: pluripotency factors as lineage specifiers. Cell Stem Cell 8, 363–369 (2011). [PubMed: 21474100]
8. Wray J et al. Inhibition of glycogen synthase kinase-3 alleviates Tcf3 repression of the pluripotency network and increases embryonic stem cell resistance to differentiation. Nat Cell Biol 13, 838–845 (2011). [PubMed: 21685889]
9. Respuela P et al. Foxd3 Promotes Exit from Naive Pluripotency through Enhancer Decommissioning and Inhibits Germline Specification. Cell Stem Cell 18, 118–133 (2016). [PubMed: 26748758]
10. Martello G et al. Esrrb is a pivotal target of the Gsk3/Tcf3 axis regulating embryonic stem cell self-renewal. Cell Stem Cell 11, 491–504 (2012). [PubMed: 23040478]
11. Leeb M, Dietmann S, Paramor M, Niwa H & Smith A Genetic exploration of the exit from self-renewal using haploid embryonic stem cells. Cell Stem Cell 14, 385–393 (2014). [PubMed: 24412312]
12. Geula S et al. Stem cells. m6A mRNA methylation facilitates resolution of naive pluripotency toward differentiation. Science 347, 1002–1006 (2015). [PubMed: 25569111]
13. Betschinger J et al. Exit from pluripotency is gated by intracellular redistribution of the bHLH transcription factor Tfe3. Cell 153, 335–347 (2013). [PubMed: 23582324]
14. Ho L & Crabtree GR Chromatin remodelling during development. Nature 463, 474–484 (2010). [PubMed: 20110991]
15. Di Croce L & Helin K Transcriptional regulation by Polycomb group proteins. Nat Struct Mol Biol 20, 1147–1155 (2013). [PubMed: 24096405]
16. Zhang Y et al. H3K36 histone methyltransferase Setd2 is required for murine embryonic stem cell differentiation toward endoderm. Cell Rep 8, 1989–2002 (2014). [PubMed: 25242323]
17. Morey L et al. Polycomb Regulates Mesoderm Cell Fate-Specification in Embryonic Stem Cells through Activation and Repression Mechanisms. Cell Stem Cell 17, 300–315 (2015). [PubMed: 26340528]
18. Aloia L et al. Zrf1 is required to establish and maintain neural progenitor identity. Genes Dev 28, 182–197 (2014). [PubMed: 24449271]
19. Morey L et al. Nonoverlapping functions of the Polycomb group Cbx family of proteins in embryonic stem cells. Cell Stem Cell 10, 47–62 (2012). [PubMed: 22226355]
20. Arai S & Miyazaki T Impaired maturation of myeloid progenitors in mice lacking novel Polycomb group protein MBT-1. EMBO J 24, 1863–1873 (2005). [PubMed: 15889154]
21. Bergemann AD, Cole F & Hirschhorn K The etiology of Wolf-Hirschhorn syndrome. Trends Genet 21, 188–195 (2005). [PubMed: 15734578]
22. Fei T et al. Smad2 mediates Activin/Nodal signaling in mesendoderm differentiation of mouse embryonic stem cells. Cell Res 20, 1306–1318 (2010). [PubMed: 21079647]
23. Wang Q et al. The p53 Family Coordinates Wnt and Nodal Inputs in Mesendodermal Differentiation of Embryonic Stem Cells. Cell Stem Cell 20, 70–86 (2017). [PubMed: 27889317]
24. Toyooka Y, Shimosato D, Murakami K, Takahashi K & Niwa H Identification and characterization of subpopulations in undifferentiated ES cell culture. Development 135, 909–918 (2008). [PubMed: 18263842]
25. Hayashi K, Ohta H, Kurimoto K, Aramaki S & Saitou M Reconstitution of the mouse germ cell specification pathway in culture by pluripotent stem cells. Cell 146, 519–532 (2011). [PubMed: 21820164]
26. Costello I et al. The T-box transcription factor Eomesodermin acts upstream of Mesp1 to specify cardiac mesoderm during mouse gastrulation. Nat Cell Biol 13, 1084–1091 (2011). [PubMed: 21822279]
27. Morrison G, Scognamiglio R, Trumpp A & Smith A Convergence of cMyc and beta-catenin on Tcf7l1 enables endoderm specification. EMBO J 35, 356–368 (2016). [PubMed: 26675138]
28. Aloia L, Di Stefano B & Di Croce L Polycomb complexes in stem cells and embryonic development. Development 140, 2525–2534 (2013). [PubMed: 23715546]
29. Kuo AJ et al. NSD2 links dimethylation of histone H3 at lysine 36 to oncogenic programming. Mol Cell 44, 609–620 (2011). [PubMed: 22099308]

30. Popovic R et al. Histone methyltransferase MMSET/NSD2 alters EZH2 binding and reprograms the myeloma epigenome through global and focal changes in H3K36 and H3K27 methylation. PLoS Genet 10, e1004566 (2014). [PubMed: 25188243]
31. Nimura K et al. A histone H3 lysine 36 trimethyltransferase links Nkx2–5 to Wolf-Hirschhorn syndrome. Nature 460, 287–291 (2009). [PubMed: 19483677]
32. Batista PJ et al. m(6)A RNA modification controls cell fate transition in mammalian embryonic stem cells. Cell Stem Cell 15, 707–719 (2014). [PubMed: 25456834]
33. Le Dily F et al. Distinct structural transitions of chromatin topological domains correlate with coordinated hormone-induced gene regulation. Genes Dev 28, 2151–2162 (2014). [PubMed: 25274727]
34. Rowley MJ & Corces VG Organizational principles of 3D genome architecture. Nat Rev Genet 19, 789–800 (2018). [PubMed: 30367165]
35. Devaiah BN et al. BRD4 is a histone acetyltransferase that evicts nucleosomes from chromatin. Nat Struct Mol Biol 23, 540–548 (2016). [PubMed: 27159561]
36. Sarai N et al. WHSC1 links transcription elongation to HIRA-mediated histone H3.3 deposition. EMBO J 32, 2392–2406 (2013). [PubMed: 23921552]
37. Filippakopoulos P et al. Selective inhibition of BET bromodomains. Nature 468, 1067–1073 (2010). [PubMed: 20871596]
38. Di Micco R et al. Control of embryonic stem cell identity by BRD4-dependent transcriptional elongation of super-enhancer-associated pluripotency genes. Cell Rep 9, 234–247 (2014). [PubMed: 25263550]
39. Hoffman JA, Wu CI & Merrill BJ Tcf7l1 prepares epiblast cells in the gastrulating mouse embryo for lineage specification. Development 140, 1665–1675 (2013). [PubMed: 23487311]
40. Wen J et al. Single-cell analysis reveals lineage segregation in early post-implantation mouse embryos. J Biol Chem 292, 9840–9854 (2017). [PubMed: 28298438]
41. Morgani SM, Metzger JJ, Nichols J, Siggia ED & Hadjantonakis AK Micropattern differentiation of mouse pluripotent stem cells recapitulates embryo regionalized cell fate patterning. Elife 7 (2018).
42. Teo AK et al. Pluripotency factors regulate definitive endoderm specification through eomesodermin. Genes Dev 25, 238–250 (2011). [PubMed: 21245162]
43. Loh KM & Lim B Epigenetics: Actors in the cell reprogramming drama. Nature 488, 599–600 (2012). [PubMed: 22932382]
44. Radzisheuskaya A et al. A defined Oct4 level governs cell state transitions of pluripotency entry and differentiation into all embryonic lineages. Nat Cell Biol 15, 579–590 (2013). [PubMed: 23629142]
45. Wamaitha SE et al. Gata6 potently initiates reprograming of pluripotent and differentiated cells to extraembryonic endoderm stem cells. Genes Dev 29, 1239–1255 (2015). [PubMed: 26109048]
46. Jaffe JD et al. Global chromatin profiling reveals NSD2 mutations in pediatric acute lymphoblastic leukemia. Nat Genet 45, 1386–1391 (2013). [PubMed: 24076604]
47. Shen C et al. NSD3-Short Is an Adaptor Protein that Couples BRD4 to the CHD8 Chromatin Remodeler. Mol Cell (2015).
48. Bennett RL, Swaroop A, Troche C & Licht JD The Role of Nuclear Receptor-Binding SET Domain Family Histone Lysine Methyltransferases in Cancer. Cold Spring Harb Perspect Med 7 (2017).
49. Rutherford EL & Lowery LA Exploring the developmental mechanisms underlying Wolf-Hirschhorn Syndrome: Evidence for defects in neural crest cell migration. Dev Biol 420, 1–10 (2016). [PubMed: 27777068]
50. Lee YF, Nimura K, Lo WN, Saga K & Kaneda Y Histone H3 lysine 36 methyltransferase Whsc1 promotes the association of Runx2 and p300 in the activation of bone-related genes. PLoS One 9, e106661 (2014). [PubMed: 25188294]
51. Gillich A et al. Epiblast stem cell-based system reveals reprogramming synergy of germline factors. Cell Stem Cell 10, 425–439 (2012). [PubMed: 22482507]

52. Ran FA et al. Genome engineering using the CRISPR-Cas9 system. Nat Protoc 8, 2281–2308 (2013). [PubMed: 24157548]
53. Aparicio-Prat E et al. DECKO: Single-oligo, dual-CRISPR deletion of genomic elements including long non-coding RNAs. BMC Genomics 16, 846 (2015). [PubMed: 26493208]
54. Di Stefano B et al. C/EBPalpha poises B cells for rapid reprogramming into induced pluripotent stem cells. Nature 506, 235–239 (2014). [PubMed: 24336202]
55. Schneider CA, Rasband WS & Eliceiri KW NIH Image to ImageJ: 25 years of image analysis. Nat Methods 9, 671–675 (2012). [PubMed: 22930834]
56. Dobin A et al. STAR: ultrafast universal RNA-seq aligner. Bioinformatics 29, 15–21 (2013). [PubMed: 23104886]
57. Schwartzman O et al. UMI-4C for quantitative and targeted chromosomal contact profiling. Nat Methods 13, 685–691 (2016). [PubMed: 27376768]
58. LI H Aligning sequence reads, clone sequences and assembly contigs with BWA-MEM. arXiv:1303.3997 (2013).
59. Bates DMM; Bolker B; Walker S Fitting Linear Mixed-Effects Models using lme4. arXiv:1406.5823 (2014).
60. Team RCR: A language and environment for statistical computing. R Foundation for Statistical Computing, Vienna, Austria. Available online at https://www.r-project.org/. (2018).
61. Stadhouders R et al. Transcription factors orchestrate dynamic interplay between genome topology and gene regulation during cell reprogramming. Nat Genet 50, 238–249 (2018). [PubMed: 29335546]
62. Org T et al. Scl binds to primed enhancers in mesoderm to regulate hematopoietic and cardiac fate divergence. EMBO J 34, 759–777 (2015). [PubMed: 25564442]
63. Alexanian M et al. A transcribed enhancer dictates mesendoderm specification in pluripotency. Nat Commun 8, 1806 (2017). [PubMed: 29180618]
64. Yu P et al. Spatiotemporal clustering of the epigenome reveals rules of dynamic gene regulation. Genome Res 23, 352–364 (2013). [PubMed: 23033340]
65. Lodato MA et al. SOX2 co-occupies distal enhancer elements with distinct POU factors in ESCs and NPCs to specify cell state. PLoS Genet 9, e1003288 (2013). [PubMed: 23437007]
66. Hailesellasse Sene K et al. Gene function in early mouse embryonic stem cell differentiation. BMC Genomics 8, 85 (2007). [PubMed: 17394647]

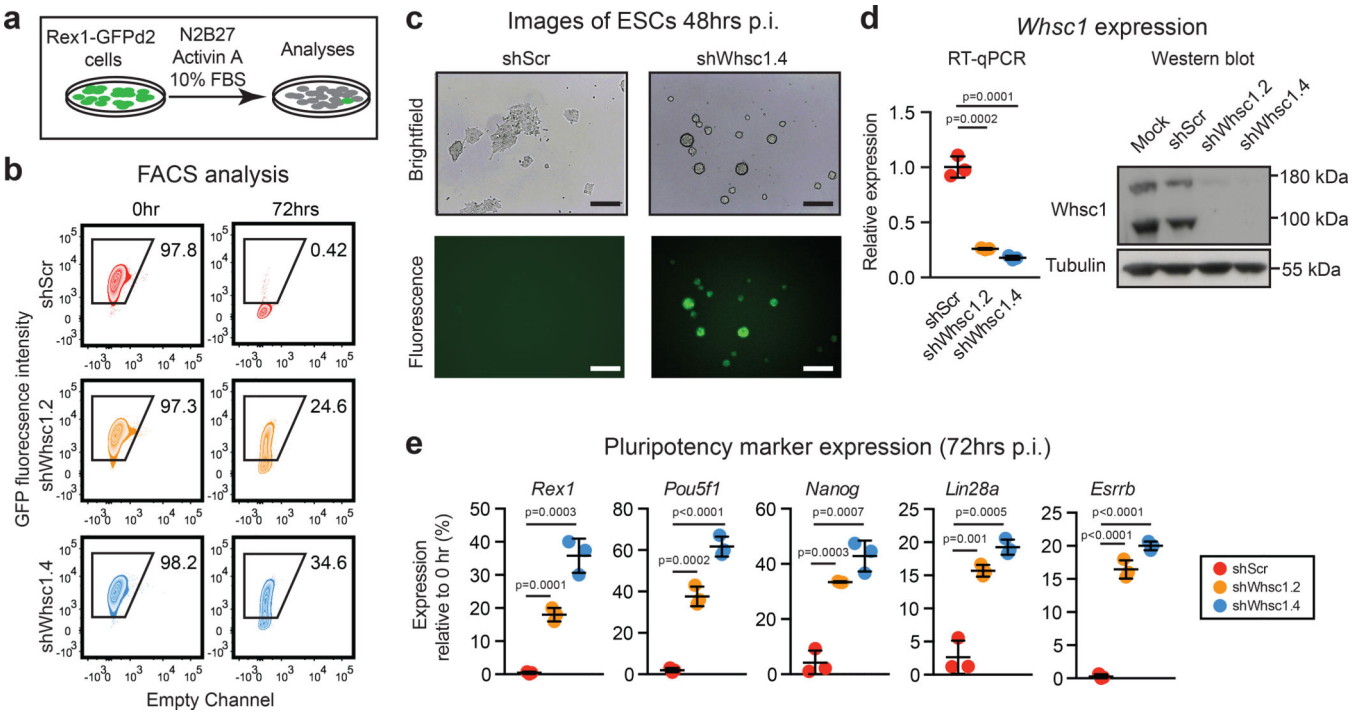

Figure 1. Whsc1 is involved in the exit from pluripotency of mESCs.

a, Experimental procedure to assess exit from pluripotency using Rex1GFPd2 ESCs. **b**, Representative FACS plots of GFP (Rex1) expression in cells expressing scrambled shRNA (shScr) as a control or shWhsc1 knockdown constructs (shWhsc1.2 and shWhsc1.4) at 0 hr and 72 hrs after induction. Three independent experiments were performed with similar results. **c**, Representative images of ESCs expressing shScr and shWhsc1.4 48 hrs after induction of exit from pluripotency. Three independent experiments were performed with similar results. Scale bar: 500 μm **d**, Expression of Whsc1 quantified by RT-qPCR (left panel) and Western blot (right panel) in control (shScr) and Whsc1 knockdown ESCs. Tubulin was used as loading control. For left panel, data represent mean±s.d. from n=3 independent experiments and p-values were calculated by two-tailed unpaired *t*-test. For right panel, three independent experiments were performed with similar results and scanned images of unprocessed blots are shown in Supplementary Fig. 8. **e**, Expression of pluripotency genes 72 hrs after induction of exit from pluripotency. Data represent mean ±s.d. from n=3 independent experiments and p-values were calculated by two-tailed unpaired *t*-test.

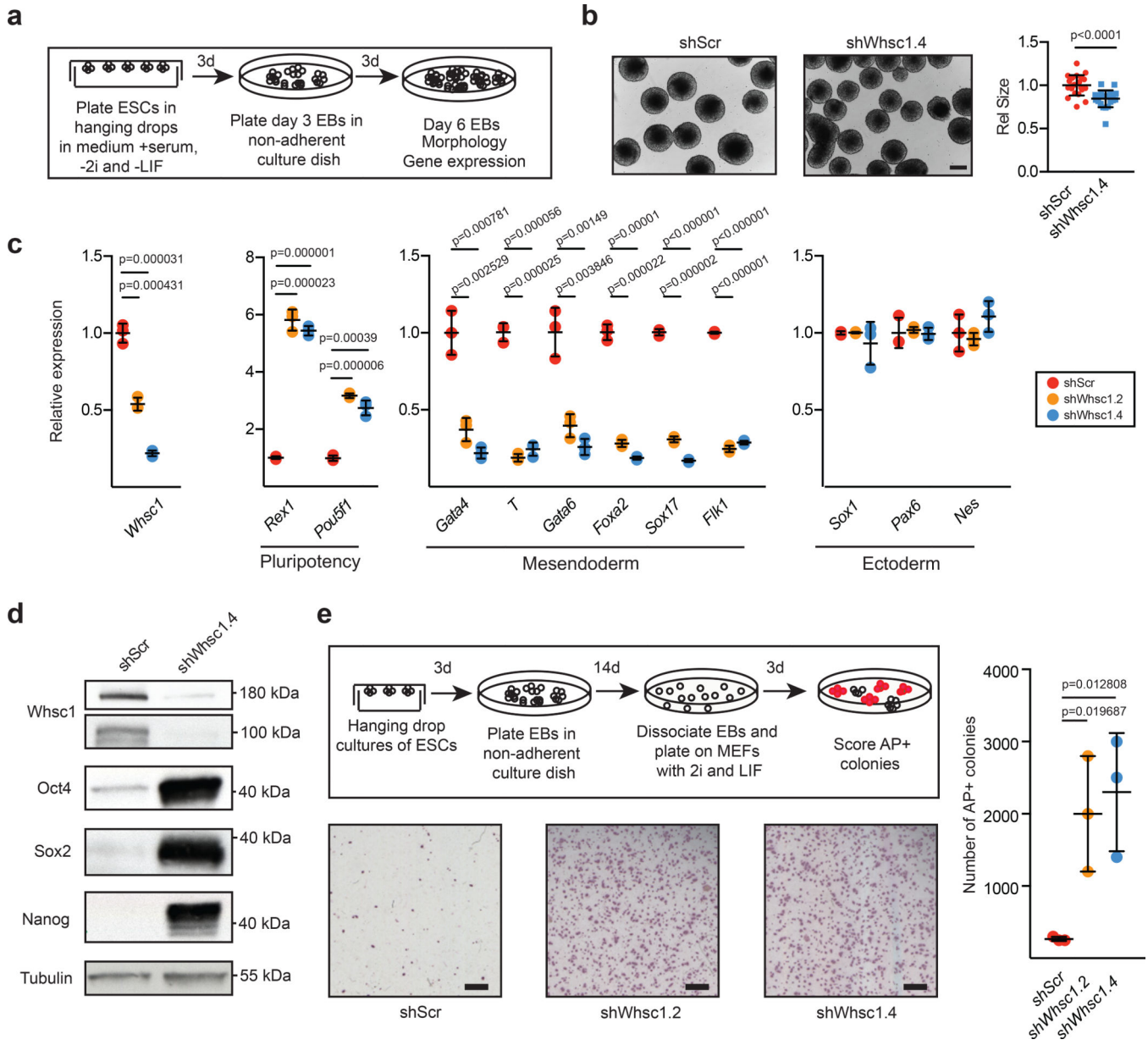

Figure 2. Whsc1 is required for mesendoderm differentiation.

a, Schematics of EB differentiation assay. **b**, Images of Day 6 EBs derived from control and Whsc1 depleted Rex1GFPd2 cells (left panel) and quantification of EB size (right panel). Data in the right panel represent mean±s.d. from shScr EBs (n=21) and shWhsc1.4 EBs (n=22) respectively. The p-value was calculated by two-tailed Mann-Whitney test. Scale Bar: 500 μm. **c**, Expression of Whsc1, pluripotency, mesendoderm and ectoderm markers in Day 6 EBs quantified by RT-qPCR from control and Whsc1 depleted Rex1GFPd2 cells. Data represent mean±s.d. from n=3 independent experiments and p-values were calculated by two-tailed unpaired *t*-test. **d**, Levels of Whsc1 and pluripotency factors in Day 6 EBs evaluated by Western Blot from control and Whsc1-depleted Rex1GFPd2 cells. Tubulin was used as loading control. Two independent experiments were performed with similar results.

Scanned images of unprocessed blots are shown in Supplementary Fig. 8. **e**, Schematics of EB re-plating assay and images of alkaline phosphatase (AP) stained colonies obtained from control and Whsc1-depleted EBs. Scale bar: 1mm; Right panel: quantification of AP positive colonies. Data represent mean±s.d. from n=3 independent experiments and p-values were calculated by two-tailed unpaired *t*-test.

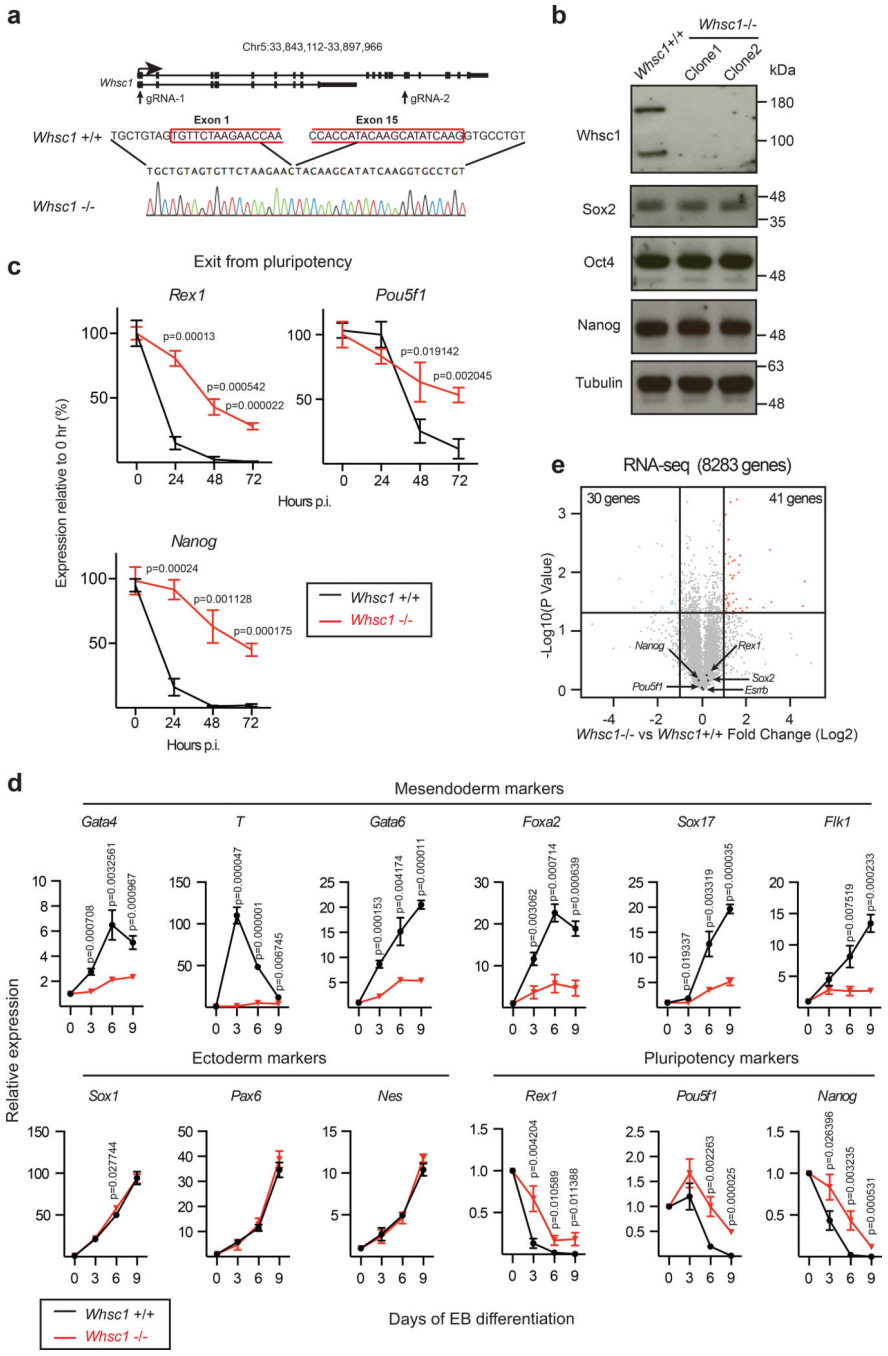

Figure 3. Ablation of *Whsc1* results in delayed down-regulation of pluripotency genes and impairment of mesendoderm formation

a, Schematics of strategy for generating ESCs with a complete *Whsc1* knockout using CRISPR-Cas9 approach. Top panel: organization of *Whsc1* that can generate two transcript isoforms (long and short). The targets of the gRNAs (exon1 and exon15) are indicated by arrows. Middle panel: genomic sequences of wild-type *Whsc1* (*Whsc1* +/+) spanning exon1 and exon 15 (exon1 and exon15 are indicated as red boxes); Bottom panel: sequence and chromatograph of the Whsc1 knockout (*Whsc1*−/−). **b**, Western blot of Whsc1 and

pluripotency factors, Sox2, Oct4 and Nanog in *Whsc1* +/+ and two *Whsc1* −/− ESC clones. Tubulin was used as loading control. Two independent experiments were performed with similar results. Scanned images of unprocessed blots are shown in Supplementary Fig. 8. **c**, Expression kinetics of pluripotency genes in *Whsc1* +/+ and *Whsc1* −/− cells were monitored by RT-qPCR after transfer into N2B27 medium containing Activin A and FBS. Data represent mean±s.d. from n=3 independent experiments and p-values were calculated by two-tailed unpaired *t*-test. **d**, Expression kinetics of mesendodermal, ectodermal and pluripotency genes were evaluated by RT-qPCR during EB formation using *Whsc1* +/+ or *Whsc1* −/− ESCs (n=3). Data represent mean±s.d. from n=3 independent experiments and p-values were calculated by two-tailed unpaired *t*-test. **e**, Volcano plot showing differentially expressed genes in *Whsc1* −/− ESCs compared to *Whsc1* +/+ ESCs. All genes with RPKM>1 were plotted and those up-regulated in *Whsc1* −/− cells were indicated as red spots (Log2FC>1 and p<0.05). Genes down-regulated in *Whsc1* −/− cells were indicated as light blue spots (Log2FC<−1 and p<0.05). Pluripotency genes, *Pou5f1, Sox2, Nanog, Esrrb and Rex1* were indicated as black spots.

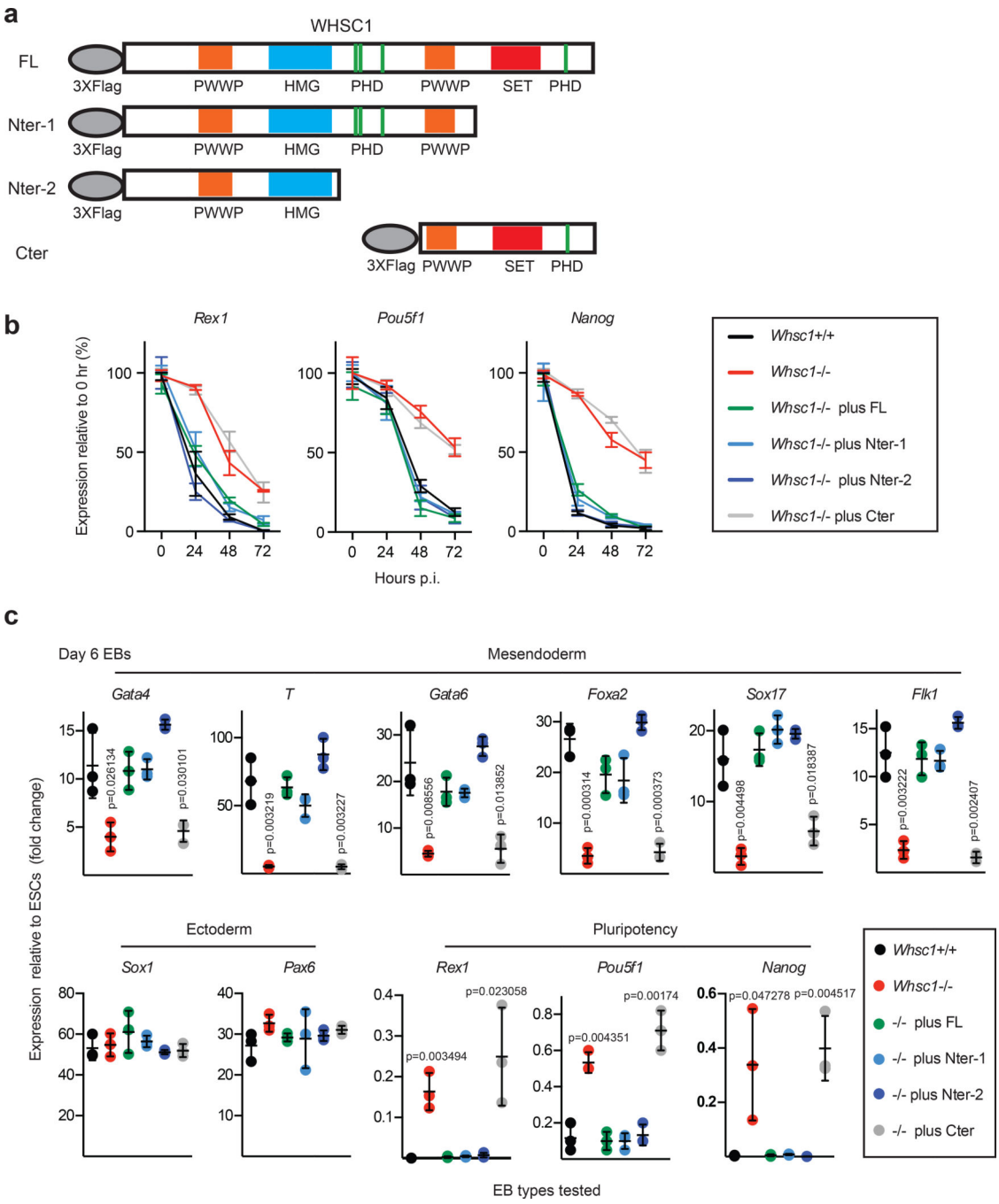

Figure 4. N-terminus of Whsc1 is sufficient to rescue pluripotency exit and mesendoderm differentiation in *Whsc1* −/− cells.

a, Schematics of full length and truncated human WHSC1 constructs tagged by 3XFlag. **b**, Expression kinetics (RT-qPCR) of pluripotency genes in *Whsc1* +/+ and in *Whsc1* −/− cells infected with WT, Nter-1, Nter-2 or Cter WHSC1 constructs after transfer into N2B27 medium containing Activin A and FBS. Data represent mean±s.d. from n=3 independent experiments. **c**, Expression of mesendodermal, ectodermal and pluripotency genes was measured by RT-qPCR in Day 6 EBs derived from *Whsc1* +/+ and *Whsc1* −/− ESCs infected

with WT, Nter-1, Nter-2 or Cter WHSC1 constructs. Data represent mean±s.d. from n=3 independent experiments and p-values were calculated by two-tailed unpaired *t*-test.

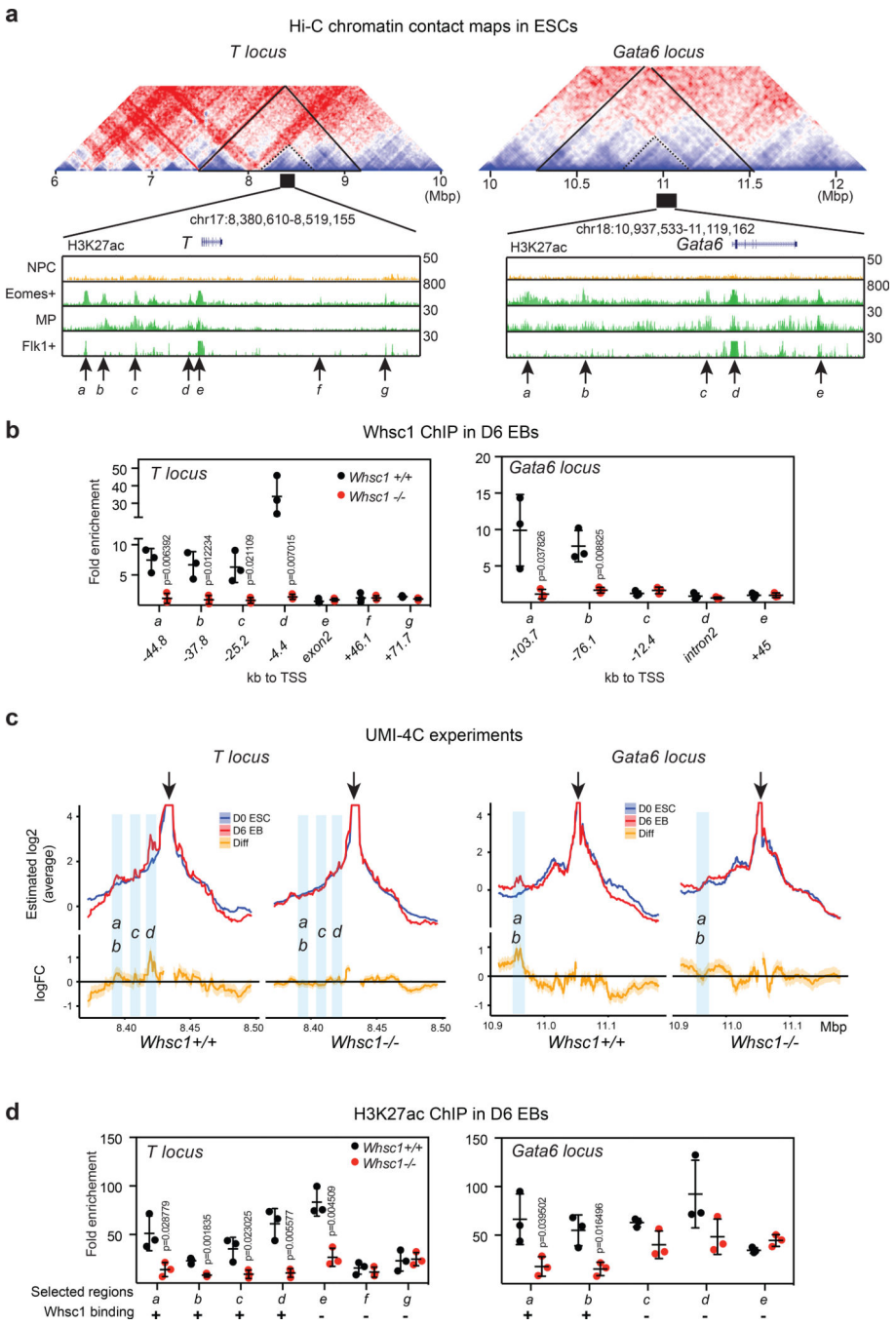

Figure 5. Whsc1 controls the enhancer activity of mesendoderm transcription factors.

a, Top panel: HiC contact maps at 10kb resolution from ESCs around *T* (Left) and *Gata6* (right) loci (GSE96611). TADs are marked by solid black lines and subTADs are indicated by dashed black lines. The regions analysed using H3K27ac ChIP-seq data are indicated as black boxes; Bottom panel: H3K27ac ChIP-seq profiles on the loci of *T* (left) *and Gata6* (right) in neural progenitor cells (NPC) (GSE35496), Eomes+ mesendodermal progenitors (GSE103262), Activin A-induced mesendodermal precursors (MP) (GSE38596) and Flk1+ mesendodermal progenitors (GSE47082). The black arrows below each panel correspond to

putative regulatory regions up or downstream of the respective gene. **b**, ChIP-qPCR quantification of Whsc1 occupancy on the same enhancers as shown in Fig. 5a above in D6 EBs from *Whsc1 +/+* and *Whsc1 −/−* cells, with numbers indicating distance to the TSS in kb. Data represent mean±s.d. from n=3 independent experiments and p-values were calculated by two-tailed unpaired *t*-test. **c**, Replicated UMI-4C profiles for baits located on the *T* (Chr17:843375) (left) and *Gata6* (Chr18:11053621) (right) promoters assayed in *Whsc1 +/+* and *Whsc1 −/−* ESCs and D6 EBs. Top panel, average contact profiles generated from the average of two independent biological replicates; bottom panel: average contact fold change D6 EBs versus D0 ESCs from two independent biological replicates. **d**, H3K27ac enrichments on putative enhancers of *T* (left) and *Gata6* (right) were quantified by ChIP-qPCR in Day 6 *Whsc1 +/+* and *Whsc1 −/−* EBs. Data represent mean±s.d. from n=3 independent experiments and p-values were calculated by two-tailed unpaired *t*-test.

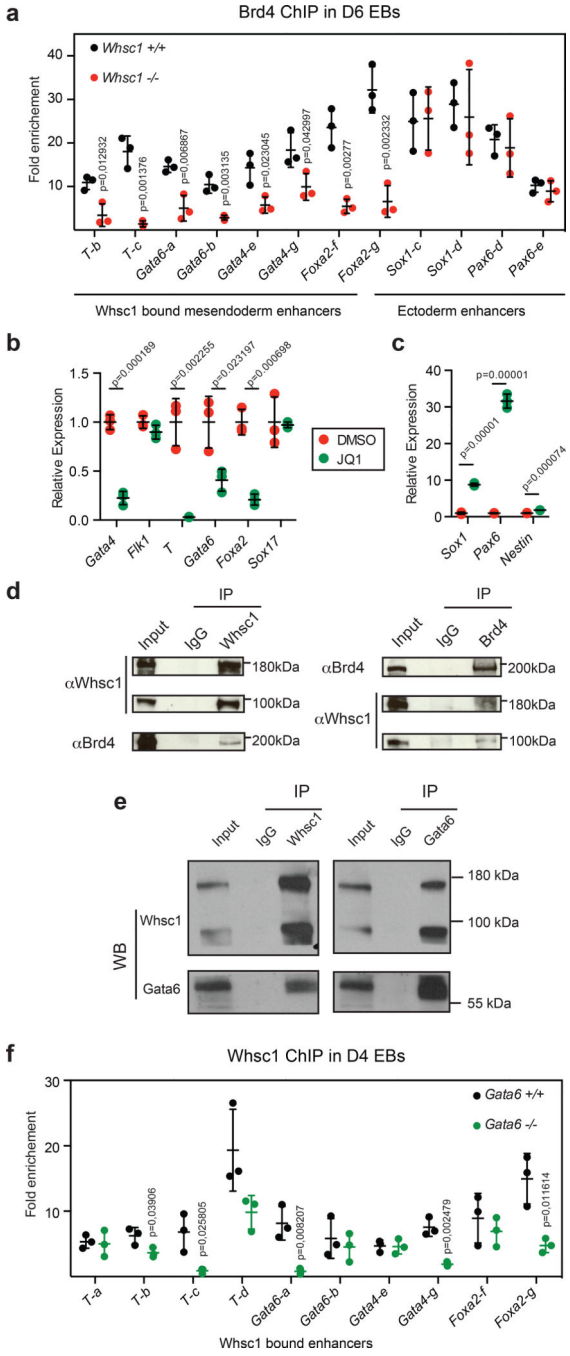

Figure 6. Whsc1 interacts with Brd4 and Gata6 on enhancers of mesendoderm transcription factors.

a, ChIP-qPCR quantification of Brd4 occupancy on Whsc1-bound putative enhancers of *T, Gata6, Gata4 and Foxa2* and control regions (*Sox1* and *Pax6*) in Day 6 *Whsc1 +/+* and *Whsc1 −/−* EBs. Data represent mean±s.d. from n=3 independent experiments and p-values were calculated by two-tailed unpaired *t*-test. **b-c**, Expression of mesendodermal markers (b) and ectodermal markers (c) quantified by RT-qPCR in Day 3 control or JQ1-treated EBs. Data represent mean±s.d. from n=3 independent experiments and p-values were calculated by two-tailed unpaired *t*-test. **d**, Western blots of endogenous Whsc1 (~180 and ~100kDa

isoforms) and Brd4 co-immunoprecipitated from total protein extracts of Day 6 EBs. Inputs correspond to 10% of total extract. Two independent experiments were performed with similar results. Scanned images of unprocessed blots are shown in Supplementary Fig. 8. **e**, Western blots of endogenous Whsc1 (~180 and ~100kDa isoforms) and Gata6 co-immunoprecipitated from total protein extracts of Day 6 EBs. Inputs correspond to 10% of total extract. Two independent experiments were performed with similar results. Scanned images of unprocessed blots are shown in Supplementary Fig. 8. **f**. ChIP-qPCR quantification of Whsc1 occupancy on Whsc1-bound putative enhancers of *T, Gata6, Gata4 and Foxa2* in Day 6 *Gata6 +/+* and *Gata6 −/−* EBs. Data represent mean±s.d. from n=3 independent experiments and p-values were calculated by two-tailed unpaired *t*-test.

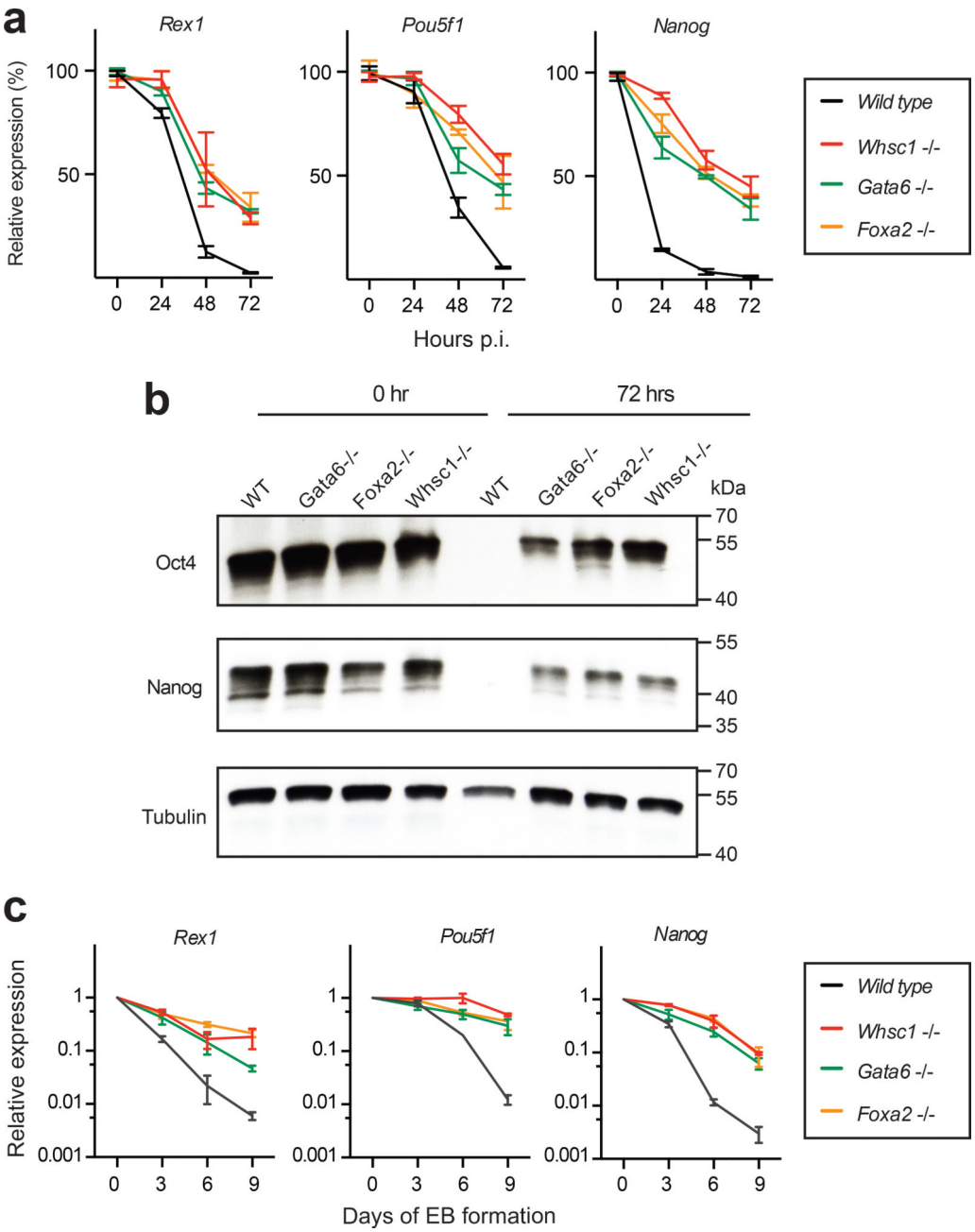

Figure 7. Mesendoderm transcription factors are required for efficient pluripotency exit.

a, Expression kinetics of pluripotency genes in *Whsc1* −/−, *Gata6* KO, *Foxa2* KO and control ESCs (WT) monitored by RT-qPCR after transfer into N2B27 medium containing Activin A and FBS Data represent mean±s.d. from n=3 independent experiments. **b**, Western blot analysis of Oct4 and Nanog in cells described in (a). Tubulin was used as loading control. Two independent experiments were performed with similar results. Scanned images of unprocessed blots are shown in Supplementary Fig. 8. **c**, Expression kinetics of pluripotency genes evaluated by RT-qPCR during EB formation using *Whsc1* −/−, *Gata6* KO

and *Foxa2* KO and control ESCs (WT). Data represent mean±s.d. from n=3 independent experiments.